Testing Matter Effects in Very Long Baseline Neutrino Oscillation Experiments

S. T. Petcov

Scuola Internazionale Superiore di Studi Avanzati, and INFN - Sezione di Trieste, I-34014 Trieste, Italy, and INRNE, Bulgarian Academy of Sciences, 1789 Sofia, Bulgaria

NEUTRINO TELESCOPES
VENICE, 6-9.3.2001

MATTER EFFECTS :

1. TEST THE MSW EFFECT

   - LMA, SMA MSW, LOW - QVO SOLUTIONS OF THE $\nu_\odot$ - PROBLEM (NOT RELEVANT IF $P_\odot(\nu_e \to \nu_e) = const$)

   - SUB-LEADING TRANSITIONS OF ν_{ATM} : $\overset{(-)}{\nu}_e \to \overset{(-)}{\nu}_{\mu(\tau)}$, $\overset{(-)}{\nu}_\mu \to \overset{(-)}{\nu}_e$;
     $\nu_\mu \cancel{\to} \nu_s$

   - SN DYNAMICS, ETC.

2. DETERMINE θ_{13}, OR OBTAIN STRINGET UPPER LIMIT ON θ_{13}

3. SIGN OF Δm^2_{ATM} :
   3-ν MIXING
   HIERARCHICAL ν- MASS SPECTRUM
   $$m_1 < m_2 \ll m_3$$

$$\Delta m^2_{ATM} = \Delta m^2_{31} > 0$$

$$\theta_{ATM} : \frac{|U_{\mu 3}|^2}{1-|U_{e3}|^2}, \quad \frac{|U_{\tau 3}|^2}{1-|U_{e3}|^2}$$

ν- MASS SPECTRUM WITH INVERTED HIERARCHY:

$m_3 \ll m_1 \cong m_2$.

$$\Delta m^2_{ATM} = \Delta m^2_{31} < 0$$

(REDEFINING THE MASSES AND $\theta_\odot$ AND θ_{ATM}: $m_1 << m_2 \cong m_3$)

RESOLVING THIS AMBIGUITY IS EXTREMELY IMPORTANT FOR, e.g., THE PREDICTIONS FOR $|<m>|$ in $(\beta\beta)_{0\nu}$-DECAY IF ν_j ARE MAJORANA PARTICLES

4. GEOPHYSICAL INFORMATION: CAN PROVIDE INFORMATION ON $\bar{N}_e$ $(= \bar{\rho}\, Y_e / M_N)$ ALONG THE ν- TRAJECTORY IN THE EARTH

5. THE STUDY OF THE CP-VIOLATION DUE TO δ_{CP} IN U_{lep} REQUIRES THE KNOWLEDGE OF THE EARTH MATTER EFFECTS IN $\nu_l \rightleftarrows \nu_{l'}$ AND $\bar{\nu}_l \rightleftarrows \bar{\nu}_{l'}$.

STUDIED BY A. DE RUJULA ET AL.,
V. BARGER ET AL., '99 -
M. FREUND ET AL., '99 -
P. LIPARI, '99
A. CERVERA ET AL., '00
M. CAMPANELLI ET AL., '00
MOCIOIU I., R. SHROCK, ...

ν - FACTORIES : $\mu^- \to e^- + \bar{\nu}_e + \nu_\mu$

$$\mu^+ \to e^+ + \nu_e + \bar{\nu}_\mu$$

MATTER EFFECTS CAN BEST BE STUDIED IN THE

$$\nu_e \to \nu_\mu$$
$$\bar{\nu}_e \to \bar{\nu}_\mu$$

$\rho_c \cong (10 - 13)\ g/cm^3$ over a distance of $R_c = 3486$ km

$\rho_m \cong (3.3 - 5.5)\ g/cm^3$ over a distance of ~2885 km

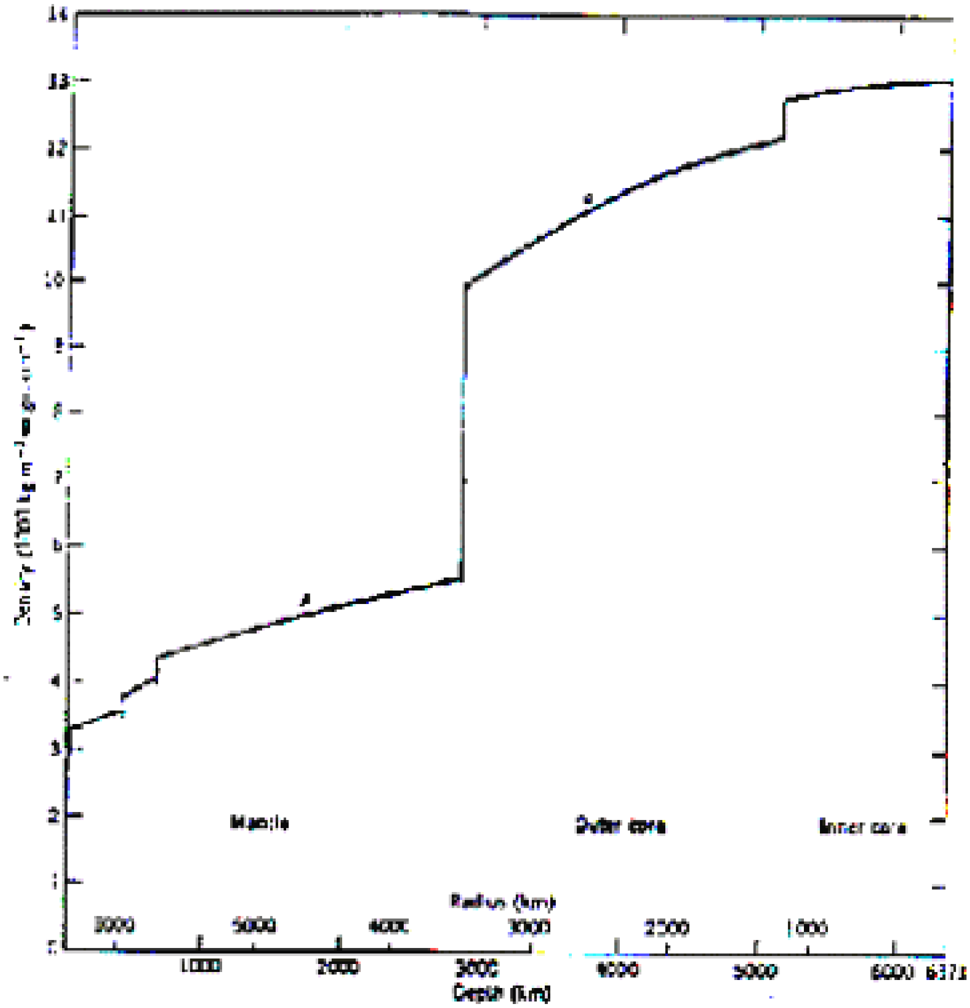

Figura 5.1: Distribuzione di densità della Terra (Stacey, 1977).

EARTH MANTLE:

$$L = 2 R_E \cos h, \quad R_E = 6371\,km$$
$$h \geq 33°, \quad L \leq 10600\,km$$

$$L = 10^3 - 10^4\,km: \quad \bar{\rho} \simeq (2.9-4.8)\,g/cm^3$$
$$Y_e = 0.494$$

Figure 1

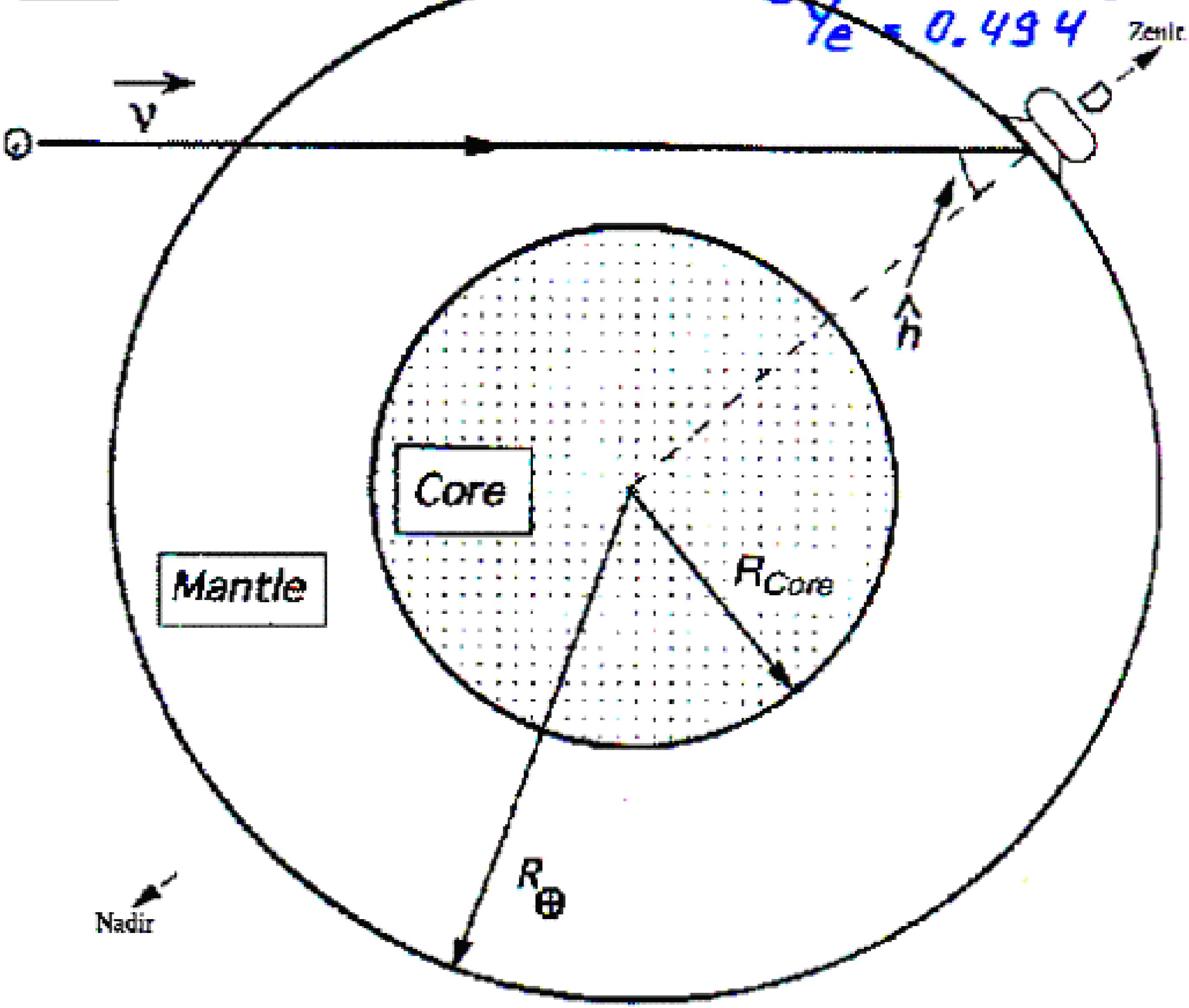

2 Three Neutrino Oscillation Probabilities in Matter

We will assume three flavour neutrino mixing:

$$|\nu_l> \;= \sum_{k=1}^{3} U_{lk}|\nu_k> \; , \qquad l = e, \mu, \tau. \tag{1}$$

where U is a 3×3 unitary matrix – the lepton mixing matrix. For our analysis we use a standard parametrization of U:

$$\begin{pmatrix} U_{e1} & U_{e2} & U_{e3} \\ U_{\mu 1} & U_{\mu 2} & U_{\mu 3} \\ U_{\tau 1} & U_{\tau 2} & U_{\tau 3} \end{pmatrix} = \begin{pmatrix} c_{12}c_{13} & s_{12}c_{13} & s_{13}e^{-i\delta} \\ -s_{12}c_{23} - c_{12}s_{23}s_{13}e^{i\delta} & c_{12}c_{23} - s_{12}s_{23}s_{13}e^{i\delta} & s_{23}c_{13} \\ s_{12}s_{23} - c_{12}c_{23}s_{13}e^{i\delta} & -c_{12}s_{23} - s_{12}c_{23}s_{13}e^{i\delta} & c_{23}c_{13} \end{pmatrix} \tag{2}$$

$c_{ij} \equiv \cos\theta_{ij}$, $s_{ij} \equiv \sin\theta_{ij}$,
δ is the Dirac CP-violation phase
$0 < \theta_{12}, \theta_{23}, \theta_{13} < \pi/2$, $0 \leq \delta < 2\pi$..

We conventionally order the masses in such a way that

$$0 < \Delta m^2_{21} < |\Delta m^2_{31}|$$

Normal neutrino mass hierarchy

$$\Delta m^2_{31} > 0 : \qquad m_3 > m_2 > m_1$$

Inverted neutrino mass hierarchy

$$\Delta m^2_{31} < 0 : \qquad m_2 > m_1 > m_3$$

which implies

$$m_2 \cong m_1 >> m_3, \quad \text{or} \quad m_2 \cong m_1 \simeq m_3$$

As long as matter and CP-violation effects are not taken into account, the two cases are phenomenologically equivalent from the point of view of neutrino oscillations.

It is natural to suppose

$$\Delta m^2_{21} = \Delta m^2_{\odot}$$

with

$$\text{LOW}-\text{QVO}: \quad 5.0 \times 10^{-10}\,\text{eV}^2 \lesssim \Delta m^2_{21} \lesssim 2.0 \times 10^{-7}\,\text{eV}^2\,, \tag{3a}$$

$$\text{SMA MSW}: \quad 4.0 \times 10^{-6}\,\text{eV}^2 \lesssim \Delta m^2_{21} \lesssim 9.0 \times 10^{-6}\,\text{eV}^2\,, \tag{3b}$$

$$\text{LMA MSW}: \quad 2.0 \times 10^{-5}\,\text{eV}^2 \lesssim \Delta m^2_{21} \lesssim 2.0 \times 10^{-4}\,\text{eV}^2\,, \tag{3c}$$

$8.0\times 10^{-4} eV^2$

Then

$$|\Delta m^2_{31}| = \Delta m^2_{\text{atm}}$$

is responsible for the dominant atmospheric $\nu_\mu \leftrightarrow \nu_\tau$ oscillations

$$\text{ATM}: \quad 10^{-3}\,\text{eV}^2 \lesssim |\Delta m^2_{31}| \lesssim 8.0 \times 10^{-3}\,\text{eV}^2 \tag{4}$$

$1.7\cdot 10^{-3}$ $\quad$ $4.0\cdot 10^{-3}$

For $E_\nu \geq 1$ GeV (1 MeV), $L \leq 10^4$ (10) km, the Δm^2-hierarchy

$$\Delta m^2_{21} \ll \Delta m^2_{31} \tag{5}$$

and

$$\Delta m^2_{21} \lesssim 10^{-4}\,\text{eV}^2,$$

the probabilities of 3-ν oscillations in vacuum reduce effectively to 2-ν vacuum oscillation probabilities

$$P^{3\nu}_{vac}(\nu_l \to \nu_{l'}) = P^{vac}(\bar{\nu}_l \to \bar{\nu}_{l'}) \cong 2|U_{l3}|^2|U_{l'3}|^2 \left(1 - \cos\frac{\Delta m^2_{31} L}{2E}\right), \quad l \neq l' = e, \mu, \tau, \tag{6}$$

$$P^{3\nu}_{\rm atm}(\nu_l \rightarrow \nu_l) = P^{3\nu}_{\rm atm}(\bar{\nu}_l \rightarrow \bar{\nu}_l) \cong 1 - 2|U_{l3}|^2(1 - |U_{l3}|^2)\ \left(1 - \cos\frac{\Delta m^2_{31} L}{2E}\right),\ l = e, \mu, \tau. \quad (7)$$

CHOOZ experiment + the oscillation interpretation of the solar and atmospheric neutrino data:

$$3.0 \times 10^{-3}\,\mathrm{eV}^2 \leq |\Delta m^2_{31}| \leq 8.0 \times 10^{-3}\,\mathrm{eV}^2 : \qquad |U_{e3}|^2 \lesssim 0.025\,,$$

$$1.0 \times 10^{-3}\,\mathrm{eV}^2 \leq |\Delta m^2_{31}| < 3.0 \times 10^{-3}\,\mathrm{eV}^2 : \qquad |U_{e3}|^2 \lesssim 0.05.$$

Under the condition (5),

$$P^{3\nu}_{MSW,VO}(\nu_e^{\odot} \rightarrow \nu_e^{\odot}) \cong |U_{e3}|^4 + (1 - |U_{e3}|^2)^2\ P^{2\nu}_{MSW,VO}(\nu_e^{\odot} \rightarrow \nu_e^{\odot}; \Delta m^2_{21}, \theta_{12})$$

where

$$\sin^2 2\theta_{12} = 4\frac{|U_{e1}|^2\,|U_{e2}|^2}{(1 - |U_{e3}|^2)^2}, \quad \cos 2\theta_{12} = \frac{|U_{e1}|^2 - |U_{e2}|^2}{1 - |U_{e3}|^2}\,, \qquad (8)$$

For $|U_{e3}|^2$ satisfying the CHOOZ limit, the dependence of $P^{3\nu}_{MSW,VO}(\nu_e^{\odot} \rightarrow \nu_e^{\odot})$ on $|U_{e3}|^2$ is rather weak and cannot be used to further constrain or determine $|U_{e3}|^2$. In general, under the condition (5) and for $\Delta m^2_{21} \lesssim 10^{-4}\,\mathrm{eV}^2$ the relevant solar neutrino transition probability depends only on the absolute values of the elements of the first row of the lepton mixing matrix, i.e., on $|U_{ei}|^2$, i=1,2,3, while the oscillations of the (atmospheric) ν_μ, $\bar{\nu}_\mu$, ν_e and $\bar{\nu}_e$ on Earth distances are controlled by the elements of the third column of U, $|U_{l3}|^2$, $l = e, \mu, \tau$. The other elements of U are not accessible to direct experimental determination.

Under the condition (5), with $\Delta m_{21}^2 \lesssim 2 \times 10^{-4}\,\mathrm{eV}^2$ and in constant density approximation,

$$P_E^{3\nu}(\nu_\mu \to \nu_e) = P_E^{3\nu}(\nu_e \to \nu_\mu) \cong s_{23}^2\; P_E^{2\nu}(\Delta m_{31}^2, \sin^2 2\theta_{13})\;, \tag{9a}$$

$$P_E^{3\nu}(\nu_\mu \to \nu_\mu) \cong c_{23}^4 + s_{23}^4\left[1 - P_E^{2\nu}(\Delta m_{31}^2, \sin^2 2\theta_{13})\right]$$
$$+\, 2c_{23}^2 s_{23}^2\left[\cos\kappa - (1 - \cos 2\theta_{13}^m)\,\sin\frac{\Delta E_m L}{2}\,\sin(\kappa + \frac{\Delta E_m L}{2})\right]\;, \tag{9b}$$

$$P_E^{3\nu}(\nu_\mu \to \nu_\tau) \cong 2c_{23}^2 s_{23}^2\left[2\sin^2\frac{\kappa}{2} - \frac{1}{2}P_E^{2\nu}(\Delta m_{31}^2, \sin^2 2\theta_{13})\right.$$
$$\left. +\,(1 + \cos 2\theta_{13}^m)\,\sin\frac{\Delta E_m L}{2}\,\sin(\kappa + \frac{\Delta E_m L}{2})\right]\;, \tag{9c}$$

where

$$P_E^{2\nu}(\Delta m_{31}^2, \sin^2 2\theta_{13}) = \frac{1}{2}\left[1 - \cos\Delta E_m L\right]\sin^2 2\theta_{13}^m \tag{10}$$

is the 2-ν transition probability in matter with constant density,

$$\kappa \cong \frac{L}{2}\left[\frac{\Delta m_{31}^2}{2E} + V - \Delta E_m\right] \tag{11}$$

is a phase, ΔE_m and θ_{13}^m are the neutrino energy difference and mixing angle in matter,

$$\Delta E_m = \frac{|\Delta m_{31}^2|}{2E}C_+,\quad \cos 2\theta_{13}^m = \frac{1}{C_+}\left(\cos 2\theta_{13} - \frac{2EV}{\Delta m_{31}^2}\right), \tag{12}$$

where

$$C_\pm^2 = \left(1 \mp \frac{2EV}{\Delta m_{31}^2}\right)^2 \pm 4\frac{2EV}{\Delta m_{31}^2}\sin^2\theta_{13} \tag{13}$$

and

$$V = \sqrt{2}G_F\bar{N}_e^{man} \tag{14}$$

is the matter term, $\bar{N}_e^{man}$ being the average electron number density along the neutrino trajectory in the earth mantle.

The probability $P_E^{3\nu}(\nu_e \to \nu_\tau)$ can be obtained from eq. (9a) by replacing the factor s_{23}^2 with c_{23}^2.

The corresponding antineutrino transition and survival probabilities have the same form and can formally be obtained from eqs. (9a–9c) by changing the sign of the matter term, i.e. $\bar{N}_e^{man} \to -\bar{N}_e^{man}$ in the expressions for κ, ΔE_m, $\cos 2\theta_{13}^m$, eqs. (11)–(12), and by replacing C_+ by C_-.

At distances $L \lesssim 6000$ km and for $\Delta m^2_{21} \sim 10^{-4}$ eV^2, the Δm^2_{21} corrections in $P^{3\nu}_E(\nu_\mu \rightarrow \nu_e)$, $P^{3\nu}_E(\nu_e \rightarrow \nu_\mu)$ and $P^{3\nu}_E(\nu_\mu \rightarrow \nu_\tau)$ can be non-negligible. It is possible to derive also the expressions for these probabilities including the leading order (CP-conserving and CP-violating) Δm^2_{21}-corrections [34]. One finds in the case of $P^{3\nu}_E(\nu_e \rightarrow \nu_\mu)$:

$$
\begin{aligned}
P^{3\nu}_E(\nu_e \rightarrow \nu_\mu) \cong\ & s^2_{23}\left[1 + \cos\delta \cot\theta_{23} \sin 2\theta'_{23}\right] P^{2\nu}_E(\,\overline{\Delta m^2_{31}}, \theta_{13}) \\
& + \ \cos\theta'_{12}\ \sin 2\theta_{23}\ \sin 2\bar{\theta}^m_{13}\ \sin\frac{\Delta \bar{E}_m L}{2} \\
& \times\ \left[\cos\delta\left(\sin(\bar{\kappa} + \frac{\Delta \bar{E}_m L}{2}) - \cos 2\bar{\theta}^m_{13} \sin\frac{\Delta \bar{E}_m L}{2}\right)\right. \\
& \left. - 2\sin\delta\ \sin\frac{\bar{\kappa}}{2}\ \sin(\frac{\bar{\kappa}}{2} + \frac{\Delta \bar{E}_m L}{2})\right]\ ,
\end{aligned}
\tag{15}
$$

where

$$
\overline{\Delta m^2_{31}} \equiv \Delta m^2_{31} - s^2_{12}\Delta m^2_{21}\ , \tag{16}
$$

$$
\bar{\kappa} = \frac{L}{2}\left[\frac{\overline{\Delta m^2_{31}}}{2E} + V - \Delta \bar{E}_m\right] - \frac{L\Delta m^2_{21}}{2E}\cos 2\theta_{12} \tag{17}
$$

and

$$
\cos\theta'_{12} = \frac{\Delta m^2_{21} c_{12} s_{12} c_{13}}{2EV + s^2_{13}\ \overline{\Delta m^2_{31}} - \Delta m^2_{21}\cos 2\theta_{12}} \cong \frac{\Delta m^2_{21} c_{12} s_{12} c_{13}}{2EV - s^2_{13}\ \Delta m^2_{31}}\ , \tag{18}
$$

$$
\sin 2\theta'_{23} = -\frac{\Delta m^2_{21}\, s_{13} \sin 2\theta_{12}}{\overline{\Delta m^2_{31}} c^2_{13} - \Delta m^2_{21}\cos 2\theta_{12}} \cong -\frac{\Delta m^2_{21}}{\Delta m^2_{31}}\, s_{13} \sin 2\theta_{12}\ . \tag{19}
$$

$P^{2\nu}_E(\,\overline{\Delta m^2_{31}}, \theta_{13})$, $\Delta \bar{E}_m$ and $\cos 2\bar{\theta}^m_{13}$ are given by (10) and (12) in which $\Delta m^2_{31} \rightarrow \overline{\Delta m^2_{31}}$. $P^{3\nu}_E(\bar{\nu}_e \rightarrow \bar{\nu}_\mu)$ ($P^{3\nu}_E(\nu_\mu \rightarrow \nu_e)$): from eq. (15) by $V \rightarrow -\ V$ and $\delta \rightarrow -\ \delta$ ($\delta \rightarrow -\ \delta$).

The terms $\sim \cos\delta$ and $\sim \sin\delta$ in eq. (15) include the leading order CP-conserving and CP-violating Δm^2_{21}–corrections, associated with the phase δ.

The expression (15) was obtained by neglecting the $\sim (\cos\theta'_{12})^2$, $(\sin 2\theta'_{23})^2$, $\cos\theta'_{12}\sin 2\theta'_{23}$ and the higher order corrections. Note that if $\Delta m^2_{21} \lesssim 2 \times 10^{-4}$ eV^2 and for $\bar{N}^{man}_e \gtrsim 1.45$ cm^{-3}N$_A$ ($L \geq 1000$ km), we have $2EV \geq 10^{-3}$ eV^2, and consequently $|\cos\theta'_{12}| \lesssim 0.1$ at $E \gtrsim 4.5$ GeV. For the indicated maximal value of Δm^2_{21} and $|\Delta m^2_{31}| \geq 10^{-3}$ eV^2, $s^2_{13} \lesssim 0.025$ (0.05) one finds $|\sin 2\theta'_{23}| \lesssim 0.032$ (0.045). Thus, if $|\Delta m^2_{31}| \cong 3.5 \times 10^{-3}$ eV^2, the correction $\sim \cos\theta'_{12}$ would be the dominant one for $E \sim (5 - 30)$ GeV.

COMMENTS:

- $P_E^{3\nu}(\overset{(-)}{\nu}_e \to \overset{(-)}{\nu}_\mu) \leq \sin^2\theta_{23} \sim 0.5$

- max $\left(P_E^{3\nu}(\nu_e \to \nu_\mu)\right) = \sin^2\theta_{23}$:

  $\sin^2 2\theta_{13}^m = 1$, $\cos \Delta E_m L = -1$

  $\sin^2\theta_{13} = 0.05\ (0.025)$, $L \geq 8 \cdot 10^3\ (10^4)$ km

- SUBSTANTIAL MATTER EFFECT IN $\overset{(-)}{\nu}_e \to \overset{(-)}{\nu}_\mu$: $E_\mu > E_{res}$

$\lvert\Delta m^2_{31}\rvert\ [10^{-3} eV^2]$	3.5	6.0	8.0
$\bar{N}_e = 2 N_A cm^{-3}$ E_{res} [GEV]	11.5	19.7	26.2

- Δm_{31} $\quad > 0 \quad\quad < 0$

	>0	<0
$\nu_e \to \nu_\mu$	ENHANCED	SUPPRESSED
$\bar{\nu}_e \to \bar{\nu}_\mu$	SUPPRESSED	ENHANCED

  $|U_{e3}|^2 \ll 1$: $\cos 2\theta_{13} > 0$

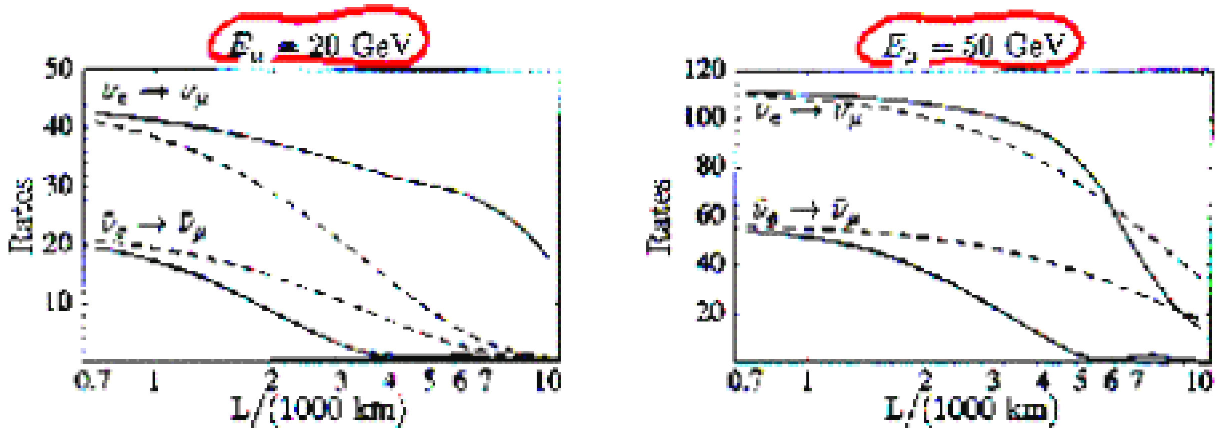

Figure 1: *Appearance event rates $n_{\mu^+}(\mu^-)$, $n_{\mu^-}(\mu^+)$ due to the $\nu_e \to \nu_\mu$ and $\bar\nu_e \to \bar\nu_\mu$ transitions in the earth mantle (solid lines) and in vacuum (dashed lines), as functions of the baseline L for $E_\mu = 20\,\mathrm{GeV}$ (left) and $E_\mu = 50\,\mathrm{GeV}$ (right). The differences between the solid and dashed lines is a measure of the magnitude of the earth matter effect. Both plots assume $N_\mu = 2 \cdot 10^{20}$, $\epsilon = 50\%$, $\sin^2 2\theta_{23} = 1$ and $\sin^2 2\theta_{13} = 0.01$. The scaling of the rates with these parameters is described in the text.*

$\Delta m^2_{31} > 0$

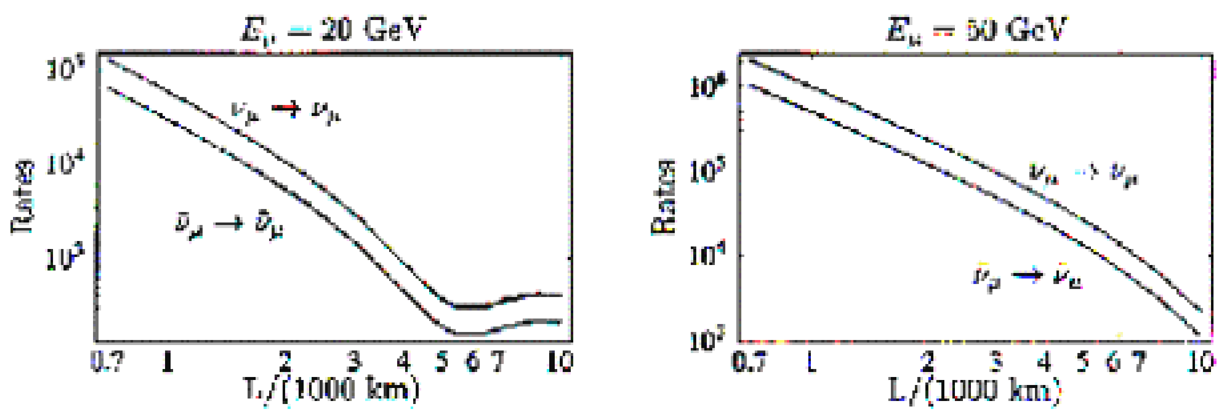

Figure 2: *Same as in fig. 1 but for the disappearance channels. The dashed lines coincide almost perfectly with the solid lines, showing that matter effects are negligible in these channels.*

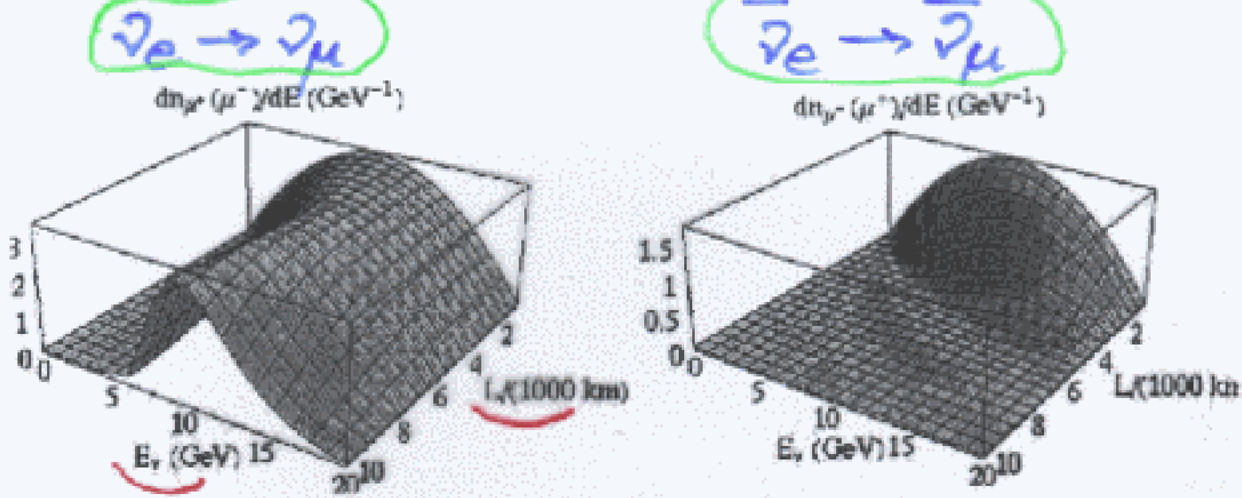

Figure 3: *Differential appearance rates for the channels $\nu_e \to \nu_\mu$ (left) and $\bar{\nu}_e \to \bar{\nu}_\mu$ (right) as functions of L and E for the same values of the parameters for which fig. 1 was obtained. The asymmetry, i.e. the enhancement of $dn_{\mu^+}(\mu^-)/dE$ and the suppression of $dn_{\mu^-}(\mu^+)/dE$, at $L \gtrsim (5000-6000)$km is related to the MSW effect (see the text).*

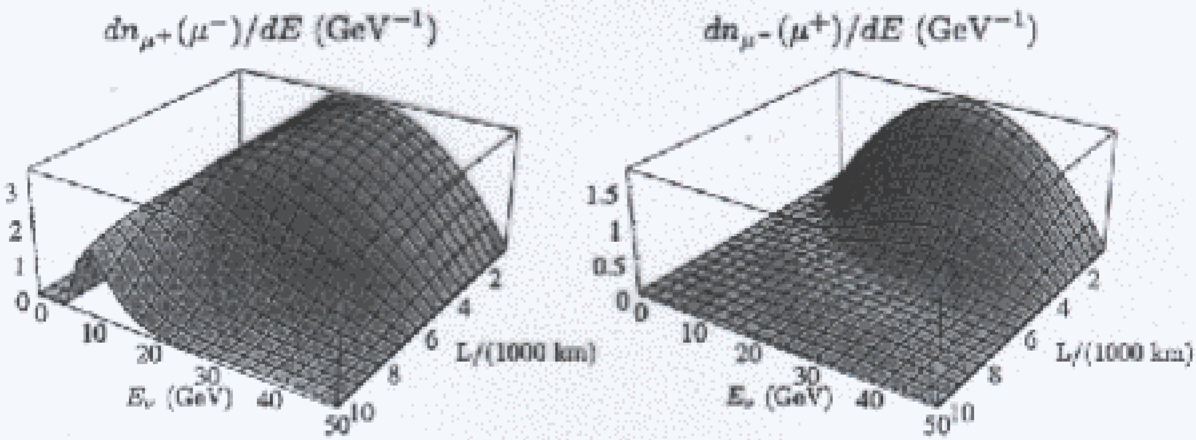

Figure 4: *Same as in fig. 3 but for a beam energy of* 50 GeV.

Figs. 3 and 4 show in more detail the differential event rates of the appearance channels $\nu_e \to \nu_\mu$ and $\bar{\nu}_e \to \bar{\nu}_\mu$ as three dimensional plots over L and E_ν. The figures show nicely the enhancement (suppression) due to the MSW mechanism in the $\nu_e \to \nu_\mu$ ($\bar{\nu}_e \to \bar{\nu}_\mu$) channel for large baseline L. To understand these figures we can look at the values of $dn_{\mu^+}(\mu^-)/dE$ and $dn_{\mu^-}(\mu^+)/dE$ for three different energies, $E = (5;\ 10;\ 15)$ GeV, and two baselines L. Specifically we compare a relatively short baseline $L = L_0 \equiv 1000$ km with a long baseline $L = 6000$ km where matter effects are more important. For $L = 1000$ km ($L = 6000$ km) the average matter electron density is $\bar{N}_e^{man} = 1.45\ \mathrm{cm}^{-3}\mathrm{N_A}$ ($\bar{N}_e^{man} \cong 2.0\ \mathrm{cm}^{-3}\mathrm{N_A}$), resulting in a resonance neutrino energy of $E_{res} = 15.8$ GeV ($E_{res} = 11.5$ GeV). The resonance energy is thus only somewhat reduced for larger baselines. The corresponding values of $\Delta_{31}(L) \equiv L\ \Delta m^2_{31}/(4E)$ and the matter effect factors C_+ and C_- which enter in $P_E^{3\nu}(\nu_e \to \nu_\mu)$ and $P_E^{3\nu}(\bar{\nu}_e \to \bar{\nu}_\mu)$ (see eqs. (9), (10), (12) and (13)) are displayed in Table 1.

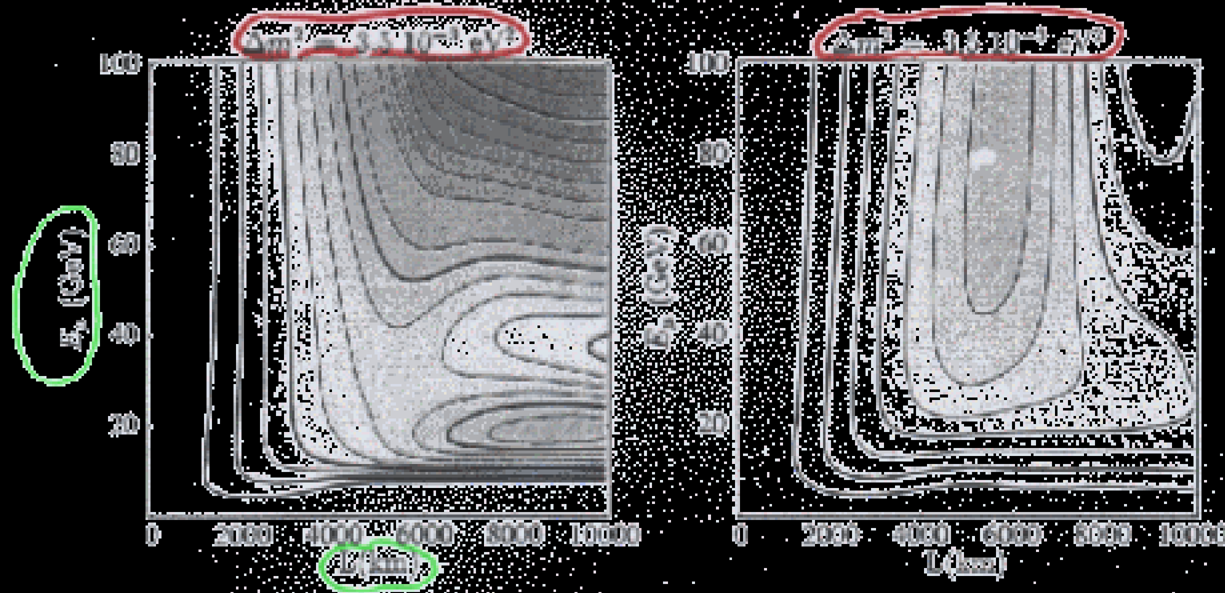

Figure 5: *Contour lines of n_e in the L-E_μ plane. We use $\Delta m^2_{21} = 3.5 \cdot 10^{-5}$ eV^2 and $N_\mu N_{KT} = 10^{21}$ and the solid contour lines correspond to $n_e = 10 \sin 2\theta_{13} \cdot \{1, 2, 4, 8, 16\}$. The left plot assumes that θ_{13} is known, while the right plot is obtained by varying θ_{13} in the range currently allowed.*

$$A = \frac{n_{\mu^+}(\mu^-) - 2n_{\mu^-}(\mu^+)}{n_{\mu^+}(\mu^-) + 2n_{\mu^-}(\mu^+)}$$

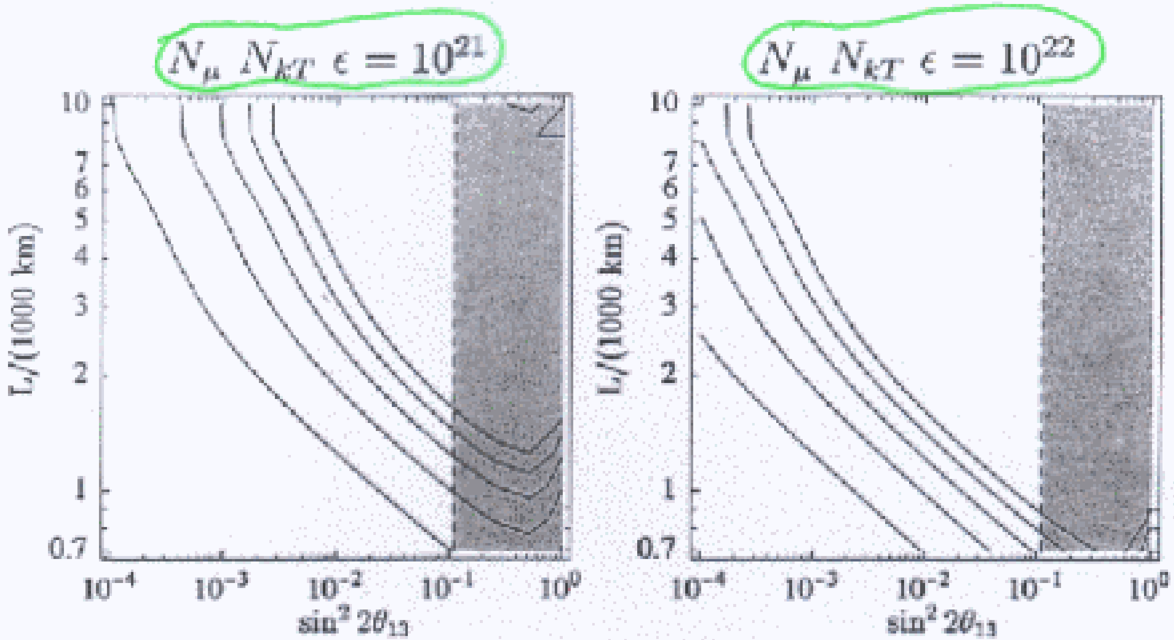

Figure 6: *Contour lines of n_σ corresponding to $n_\sigma = 1, 2, 3, 4, 5$ in the $\sin^2 2\theta_{13}$-L plane for $E_\mu = 20\,\mathrm{GeV}$ and the two different values $N_\mu N_{kT}\epsilon = 10^{21}$ (left plot) and $N_\mu N_{kT}\epsilon = 10^{22}$ (right plot).*

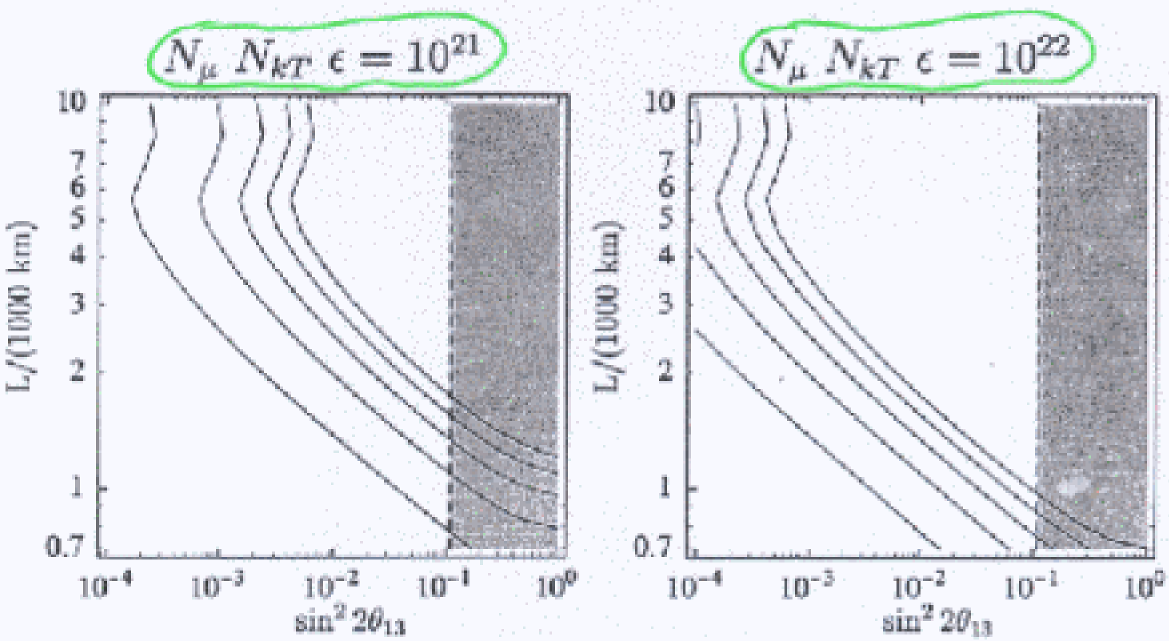

Figure 7: *Same as in fig. 6 but for* $E_\mu = 50\,\mathrm{GeV}$.

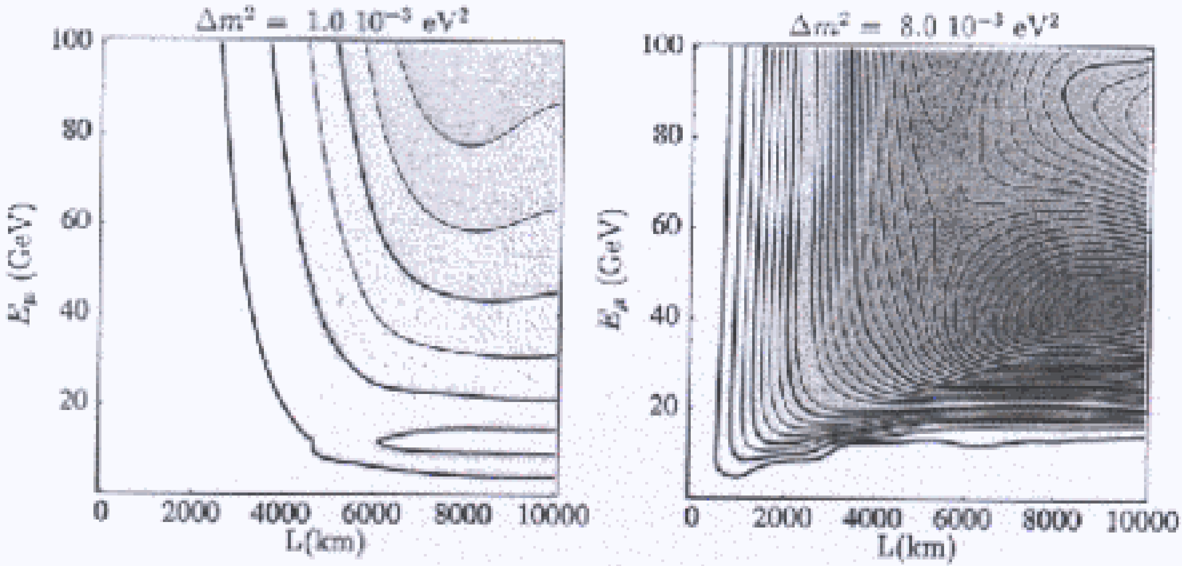

Figure 8: *Sensitivity of the statistical significance of matter effects to the value of Δm^2_{31} analogous to fig. 5. The left plot uses $\Delta m^2_{31} = 1.0 \cdot 10^{-3}\,\mathrm{eV}^2$ while for the right plot $\Delta m^2_{31} = 8.0 \cdot 10^{-3}\,\mathrm{eV}^2$ with otherwise unchanged parameters. As in fig. 5 the solid contour lines correspond to $n_\sigma = 10 \sin 2\theta_{13} \cdot \{1, 2, 4, 8, 16\}$.*

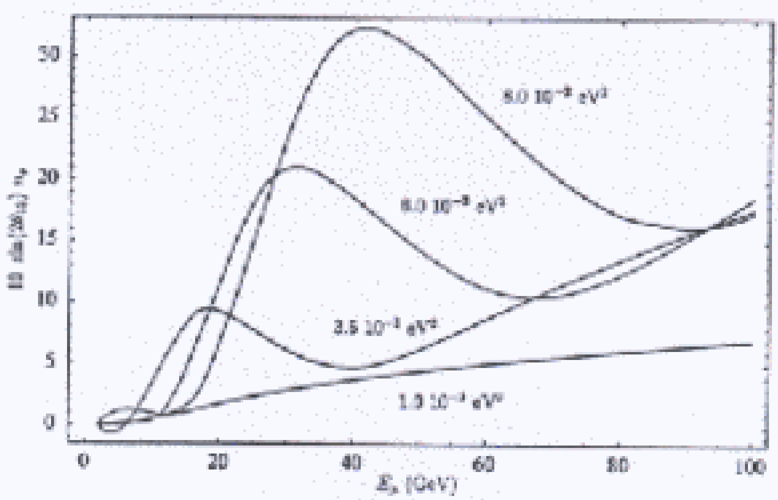

Figure 9: *Sensitivity of the statistical significance of matter effects to the value of Δm^2_{31} for fixed $L = 8000$ km as a function of E_μ. The lines show $10 \sin 2\theta_{13} n_\sigma$ for different Δm^2_{31} values.*

5 Subleading Δm^2_{21}-effects

The LMA MSW solution: $\Delta m^2_{21} \lesssim 2 \cdot 10^{-4}\,\mathrm{eV}^2$, $\sin^2 2\theta_{12} \sim 0.8$.

Effects associated to Δm^2_{21} can become important.

If Δm^2_{21} is non-negligible, θ_{12} and δ become relevant: $\theta_{12} = \theta_{\odot}^{LMA}$, $0 \leq \delta < 2\pi$.

In the following numerical results we use $\sin^2 2\theta_{12} = 0.8$ $\Delta m^2_{21} = 0$ (solid line), $\delta = 0,\ \pi/2,\ \pi,\ 3\pi/2$ (dashed lines), $\sin^2 2\theta_{13} = 0.1;\ 0.01$, $N_\mu N_{kT} \epsilon = 10^{21}$.

The size of the Δm^2_{21} effects depends crucially on the value of θ_{13}.

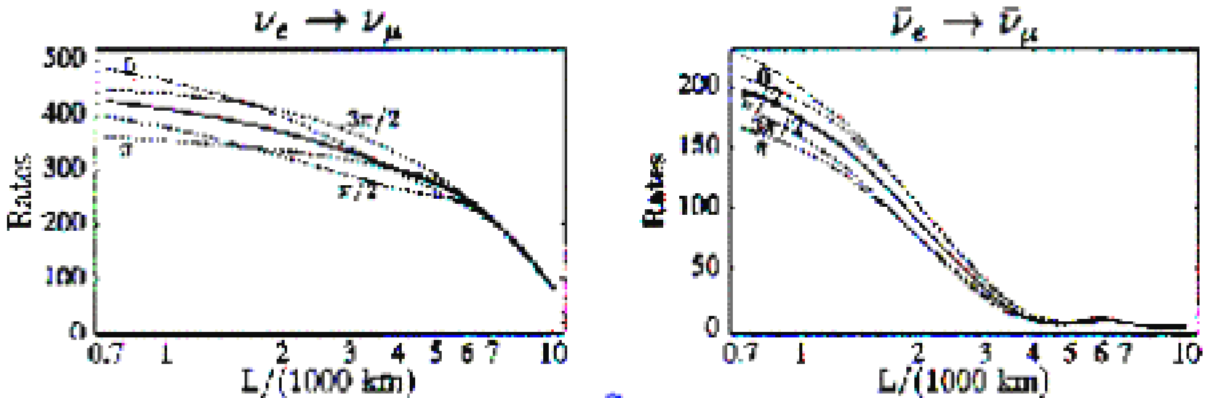

$\Delta m^2_{21} = 10^{-4}\,eV^2$

Figure 10: *Appearance event rates $n_{\mu^-}(\mu^-)$, $n_{\mu^+}(\mu^+)$ in matter with subleading $\Delta m^2_{21} = 10^{-4}\,\mathrm{eV}^2$ and four possible values of the CP-phase $\delta = 0,\ \pi/2,\ \pi,\ 3\pi/2$ against baseline L (dashed lines) compared with the corresponding event rates with negligible Δm^2_{21} (solid lines) for the channels $\nu_e \to \nu_\mu$ (left) and $\bar\nu_e \to \bar\nu_\mu$ (right). Both figures correspond to $N_\mu = 2 \cdot 10^{20}$, $\epsilon = 50\%$, $E_\mu = 20\,\mathrm{GeV}$, $\sin^2 2\theta_{23} = 1$, $\sin^2 2\theta_{12} = 0.8$ and $\sin^2 2\theta_{13} = 0.1$.*

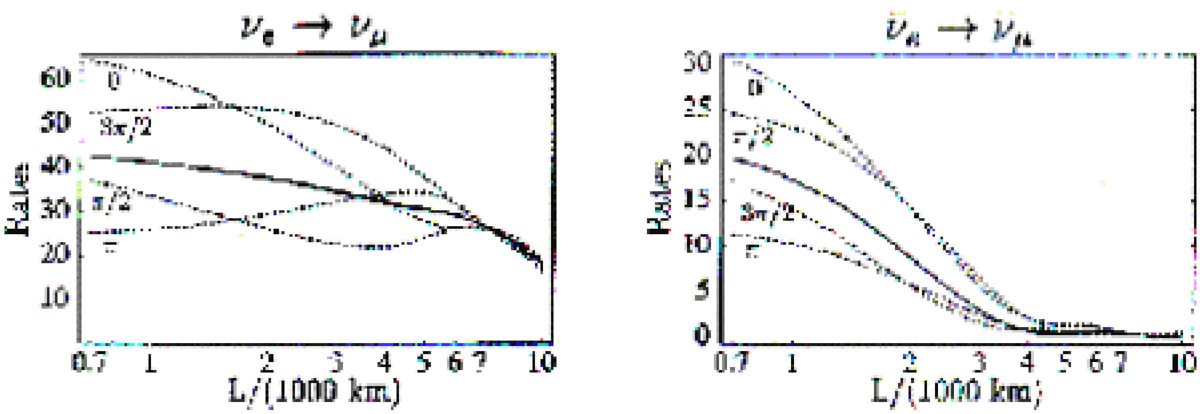

Figure 11: *Same as fig. 10 but for $\sin^2 2\theta_{13} = 0.01$.*

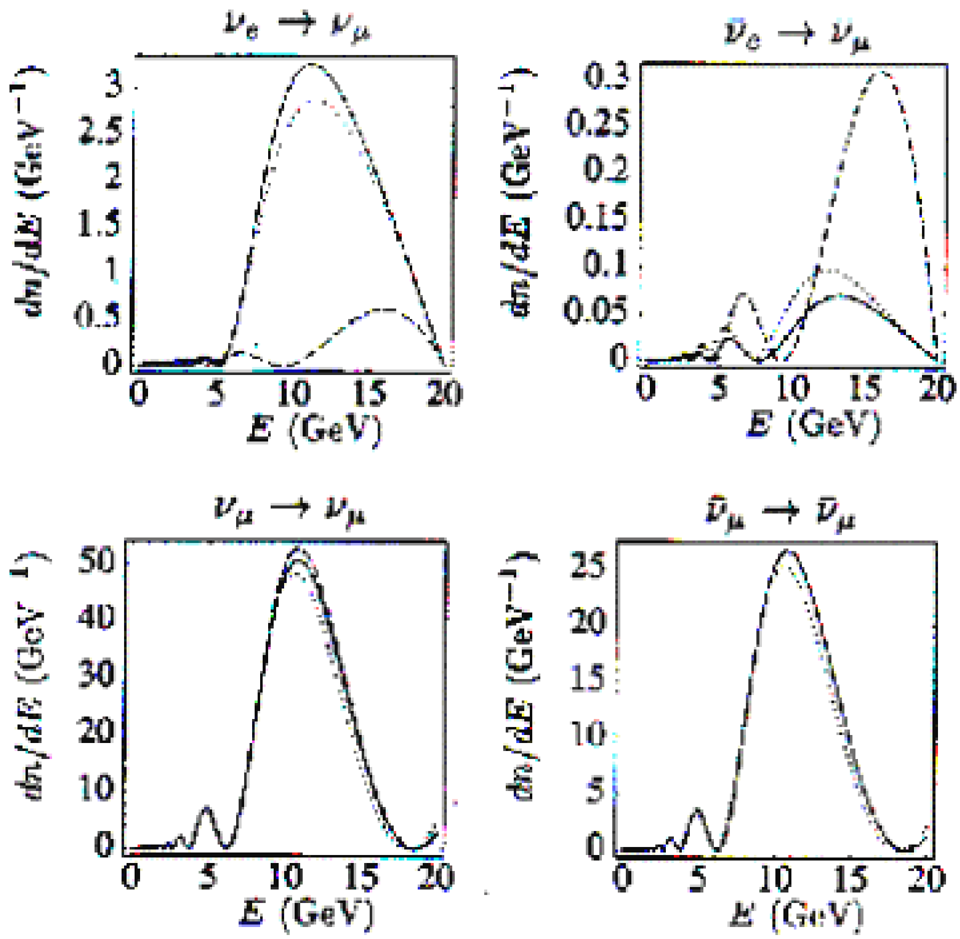

Figure 12: *Modifications in the differential event rate spectrum (events per GeV) due to matter effects for $E_\mu = 20\,\mathrm{GeV}$. The solid lines correspond to oscillations taking place in the earth mantle, while the dashed lines are for oscillations in vacuum, with $\Delta m^2_{21} = 0$ in both cases. The "enhancement", the "broadening" and the "shift" of the first oscillation maximum in the $\nu_e \to \nu_\mu$ channel as E decreases, caused by the MSW effect, is clearly seen. The dotted lines show for comparison an example of Δm^2_{21} corrections for $\Delta m^2_{21} = 10^{-4}\ \mathrm{eV}^2$, $\delta = 0$ and $\sin^2 2\theta_{12} = 0.8$. The assumed parameters are in all cases $N_\mu N_{kT} = 10^{21}$, $L = 6586$ km (CERN-MINOS), $\Delta m^2_{31} = 3.5x10^{-3}\ \mathrm{eV}^2$ and $\sin^2 2\theta_{13} = 0.01$.*

7 Matter Effects in the Energy Spectrum.

The MSW effect changes the probabilities compared to vacuum in three genuine ways: The first maximum of the oscillation probability as the energy decreases is enhanced, its width is broadened and its center is shifted to lower energies. Similarly one has an "anti-MSW effect" in the antineutrino appearance channel which implies for the first oscillation maximum a reduction in height, again a broadening and a shift to lower energies.

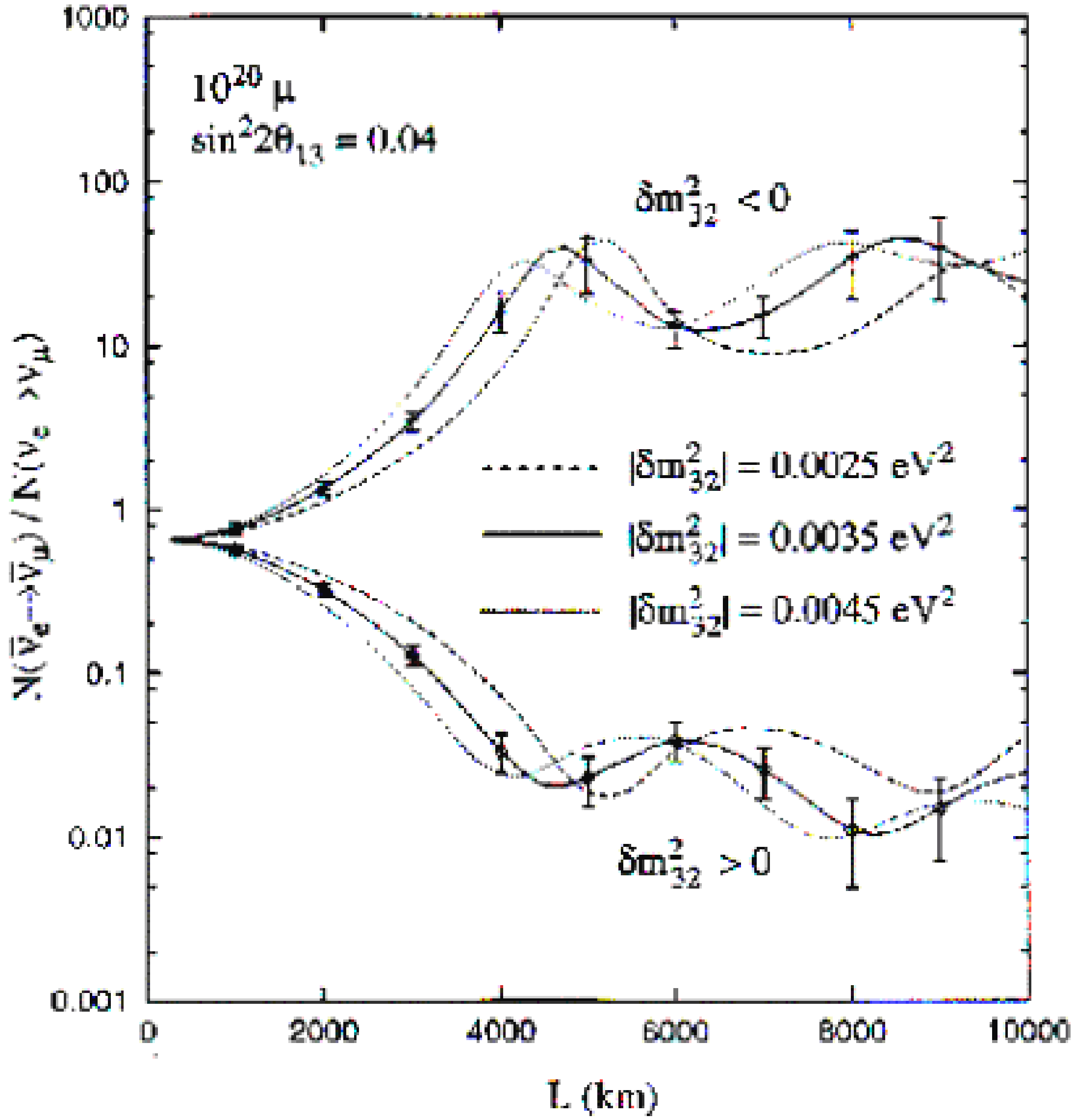

Figure 1: The ratio of wrong-sign muon event rates $N(\bar{\nu}_e \to \bar{\nu}_\mu)/N(\nu_e \to \nu_\mu)$ versus baseline for a 20 GeV muon storage ring and $\delta m^2_{32} = 0.0025$ eV^2 (dashed line), 0.0035 eV^2 (solid line), and 0.0045 eV^2 (dotted line). The other oscillation parameters are given in Eq. (1). A 4 GeV minimum cut was imposed on the detected muon energy. The error bars show the statistical errors corresponding to 10^{20} decays and a 50 kiloton detector.

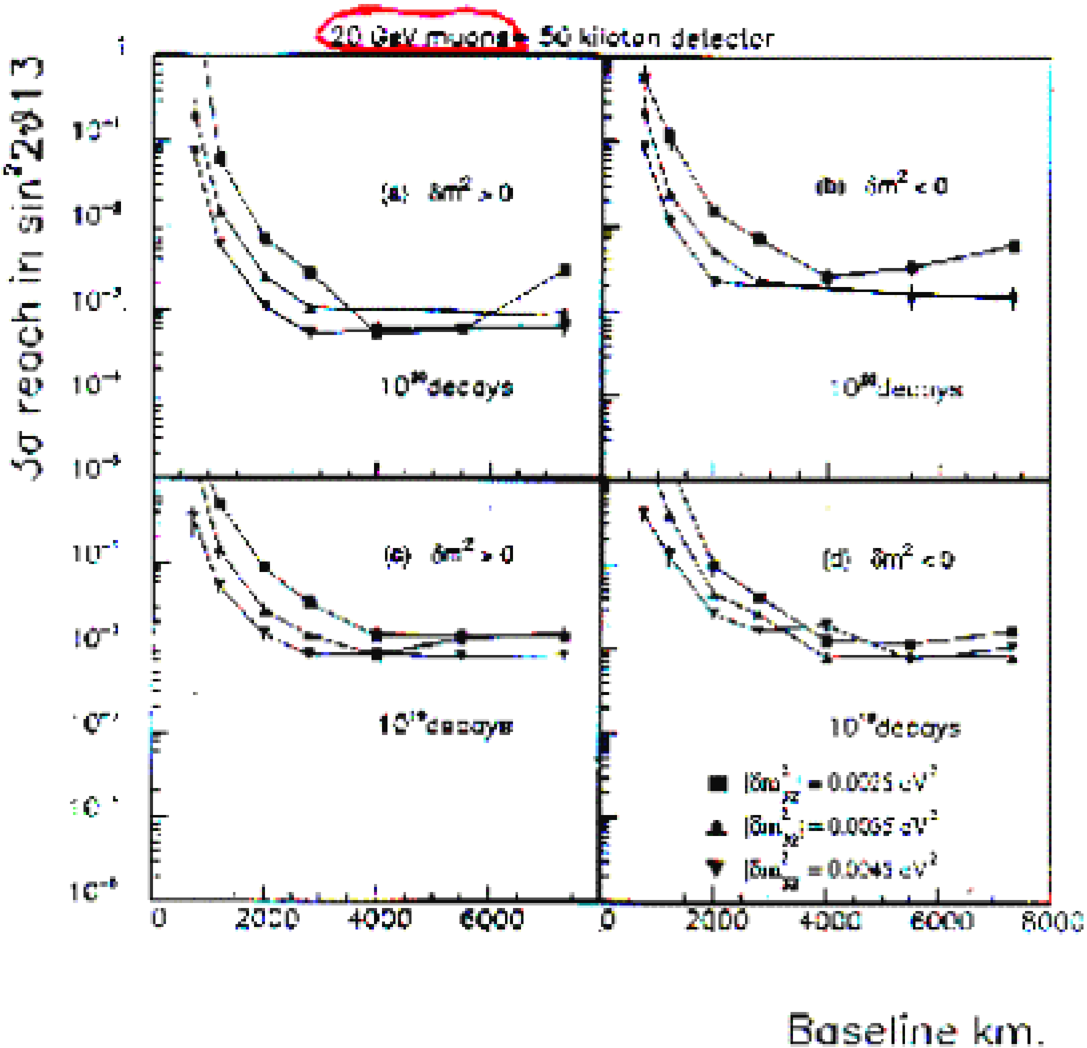

Figure 4: The minimum value of $\sin^2 2\theta_{13}$ for which the sign of δm^2_{32} can be determined to at least 3 standard deviations versus baseline length for various values of δm^2_{32}. The results are shown for a 50 kiloton detector and (a) 10^{20} μ^+ and μ^- decays and positive values of δm^2_{32}; (b) 10^{20} μ^+ and μ^- decays and negative values of δm^2_{32}; (c) 10^{19} μ^+ and μ^- decays and positive values of δm^2_{32}; (d) 10^{19} μ^+ and μ^- decays and negative values of δm^2_{32}.

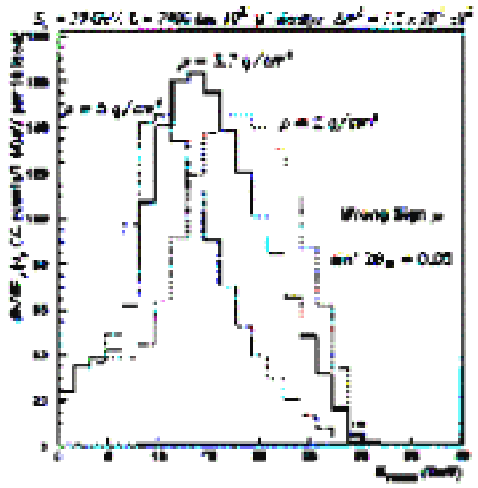

Figure 10: Variation of the MSW resonance peak for wrong sign muons as a function of Earth's density. The plot is normalized to 10^{21} μ^- decays.

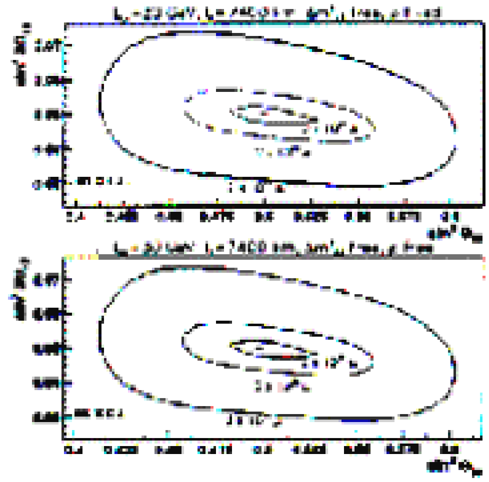

Figure 11: 68%C.L. two-dimensional contours for $\sin^2 2\theta_{13}$ and $\sin^2 \theta_{23}$: influence of ρ in the determination of the mixing angles for three different muon normalizations and $L = 7400$ km. In the upper plot ρ is fixed during the fit, while in the lower one is taken as a free parameter.

(M. CHIZHOV, S.T.P. '99)

$\nu_e \to \nu_\mu : h = 0^\circ$

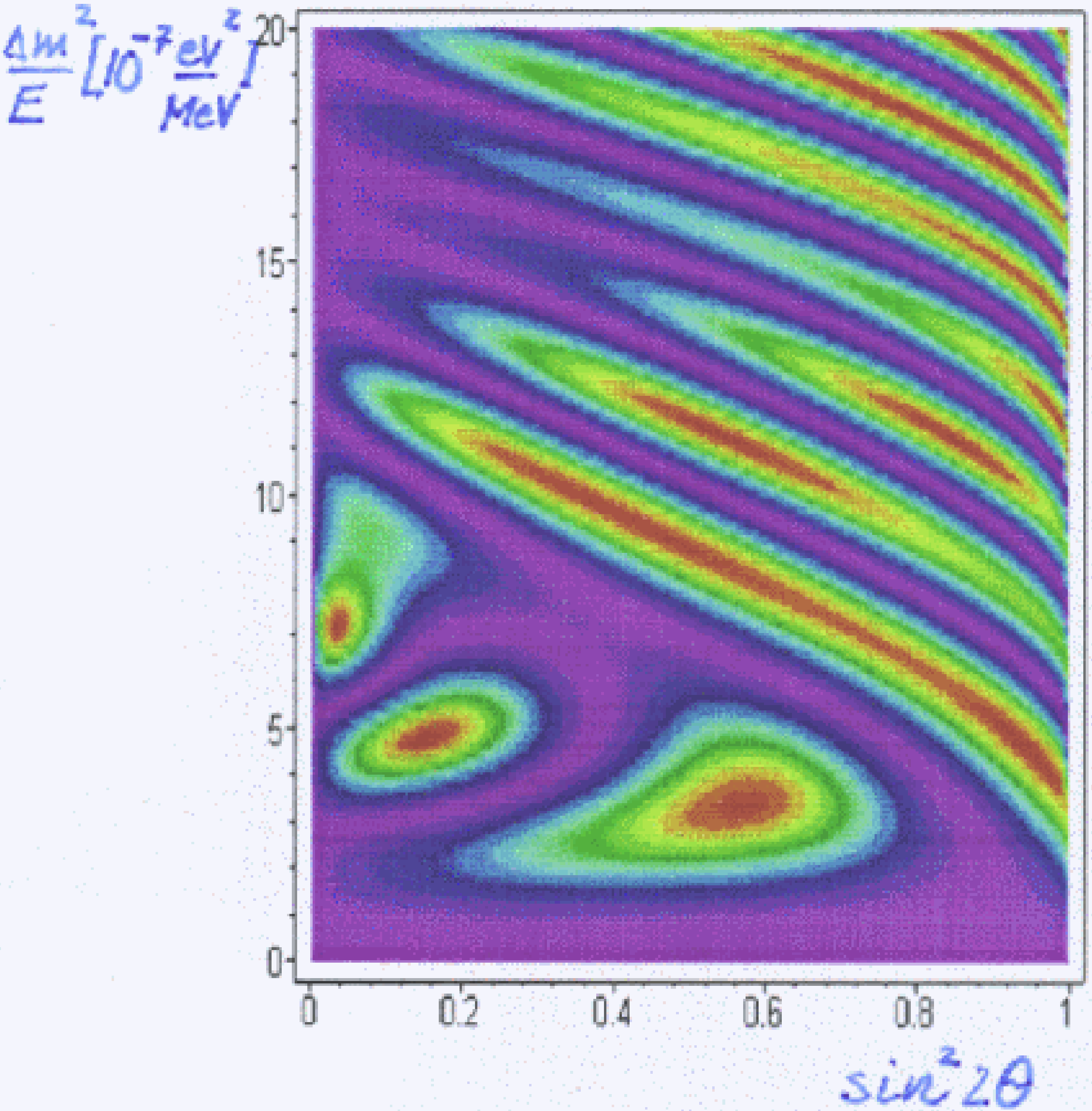

Based on : S.T.P., Phys. Lett. B434 ('98) 321;

Hep-ph/9809587 (J'98)
SISSA 108/98/EP

Hep-ph/9811205
SISSA 111/98/EP

M. Chizhov, M. Maris, S.T.P.
SISSA 53/98/EP, 31.7.'98
Hep-ph/9810501.

See also: M. Maris, S.T.P., PR D56 ('97) 7444
PR D58 ('98)

(D-N effect) Q.Y. Liu, M. Maris, S.T.P., PR D56 ('97) 5991

M. Chizhov, S.T.P.
SISSA 29/99/EP, hep-ph/9903399
SISSA 28/99/EP, hep-ph/9903424
Phys. Rev. Lett. 83 ('99) 1906

M. Maris, S.T.P., PR D62 (2000) 093006
(hep-ph/0003301);
hep-ph/0004151

CONCLUSIONS

ν - FACTORIES HAVE ENORMOUS POTENTIAL FOR STUDIES OF ν - OSCILLATIONS AND LEPTON MIXING

CAN BE FULLY EXPLOITED IF THE LMA MSW SOLUTION OF THE $\nu_\odot$ - PROBLEM IS THE TRUE ONE,

AND $\Delta m^2_{21} \gtrsim 10^{-4} eV^2$.

FOR ANY $\Delta m^2_{21} = \Delta m^2_\odot$.

THE MATTER EEEFCTS CAN BE OBSERVED FOR $\sin^2 2\theta_{13} \gtrsim (5 \cdot 10^{-4} - 10^{-3})$;
sign (Δm^2_{31}) can be determined,
INFORMATION ABOUT N_e CAN BE OBTAINED
θ_{13} AND Δm^2_{31}, θ_{23} CAN BE MEASURED WITH HIGH PRECISION.

$E_\mu \sim 20$; or 50 GeV

$L \sim 7000$ km

SUBJECT TO FURTHER STUDIES.